EJN European Journal of Neuroscience

FENS Federation of European Neuroscience Societies

European Journal of Neuroscience, Vol. 42, pp. 1818–1829, 2015 doi:10.1111/ejn.12945

MOLECULAR AND SYNAPTIC MECHANISMS

Heterogeneous effects of antiepileptic drugs in an *in vitro* epilepsy model – a functional multineuron calcium imaging study

Yoshie Hongo,[1] Keiko Takasu,[1] Yuji Ikegaya,[2,3] Minoru Hasegawa,[1] Gaku Sakaguchi[1] and Koichi Ogawa[1]

[1]Pain & Neuroscience, Discovery Research Laboratory for Core Therapeutic Areas, Shionogi Co. Ltd., 1-1 Futaba-cho 3-chome, Toyonaka, Osaka 561-0825, Japan

[2]Laboratory of Chemical Pharmacology, Graduate School of Pharmaceutical Sciences, University of Tokyo, Bunkyo-ku, Tokyo, Japan

[3]Center for Information and Neural Networks, Suita City, Osaka, Japan

Keywords: antiepileptic drugs, hippocampus, seizure-like events, synchronous Ca^{2+} influx

Abstract

Epilepsy is a chronic brain disease characterised by recurrent seizures. Many studies of this disease have focused on local neuronal activity, such as local field potentials in the brain. In addition, several recent studies have elucidated the collective behavior of individual neurons in a neuronal network that emits epileptic activity. However, little is known about the effects of antiepileptic drugs on neuronal networks during seizure-like events (SLEs) at single-cell resolution. Using functional multineuron Ca^{2+} imaging (fMCI), we monitored the activities of multiple neurons in the rat hippocampal CA1 region on treatment with the proconvulsant bicuculline under Mg^{2+}-free conditions. Bicuculline induced recurrent synchronous Ca^{2+} influx, and the events were correlated with SLEs. Other proconvulsants, such as 4-aminopyridine, pentetrazol, and pilocarpine, also induced synchronous Ca^{2+} influx. We found that the antiepileptic drugs phenytoin, flupirtine, and ethosuximide, which have different mechanisms of action, exerted heterogeneous effects on bicuculline-induced synchronous Ca^{2+} influx. Phenytoin and flupirtine significantly decreased the peak, the amount of Ca^{2+} influx and the duration of synchronous events in parallel with the duration of SLEs, whereas they did not abolish the synchronous events themselves. Ethosuximide increased the duration of synchronous Ca^{2+} influx and SLEs. Furthermore, the magnitude of the inhibitory effect of phenytoin on the peak synchronous Ca^{2+} influx level differed according to the peak amplitude of the synchronous event in each individual cell. Evaluation of the collective behavior of individual neurons by fMCI seems to be a powerful tool for elucidating the profiles of antiepileptic drugs.

Introduction

Epilepsy is a chronic brain disease characterised by recurrent seizures. Synchronous activation of neuronal networks caused by disruption of the excitatory–inhibitory balance is thought to be important for the pathogenic mechanism. There have been many studies of *in vitro* epilepsy models, using proconvulsants (Avoli *et al.*, 1993; Borck & Jefferys, 1999), electrical induction (Stasheff *et al.*, 1985), and changes in the extracellular ionic environment, such as low Ca^{2+} (Jefferys & Haas, 1982; Taylor & Dudek, 1982), low Mg^{2+} (Anderson *et al.*, 1986; Mody *et al.*, 1987), and high K^{+} (Korn *et al.*, 1987; Traynelis & Dingledine, 1988). Seizure-like events (SLEs) are seen as hallmarks in these *in vitro* models, and are identified as sustained synchronous oscillations in local field potential recordings (Anderson *et al.*, 1986; Nyikos *et al.*, 2003). These studies have revealed important aspects of the properties and mechanisms of seizures. In addition, the effects of various antiepileptic drugs have been investigated in these models (Fueta & Avoli, 1992; Leschinger *et al.*, 1993; Albus *et al.*, 2012).

Most of the studies cited above were performed with electrophysiological techniques, and they focused on the local activities of neuronal networks, such as a few cells or several regions. However, these studies did not provide information about the collective behavior of individual neurons in a neuronal network with epileptic activity. The central nervous system consists of numerous cells that act in a cooperative manner. Therefore, monitoring the collective behavior of a large-scale network at single-cell resolution is important to gain a better understanding of the pathological condition.

To address this issue, functional multineuron Ca^{2+} imaging (fMCI) has been developed as a technique for neural network imaging at single-cell resolution in recent decades (Smetters *et al.*, 1999; Cossart *et al.*, 2005; Takahashi *et al.*, 2007, 2010). Many studies have made use of fMCI to probe the dynamics of neuronal circuits (Cossart *et al.*, 2003; Ikegaya *et al.*, 2004; Sasaki *et al.*, 2007; Bonifazi *et al.*, 2009). Epilepsy in the cortex and hippocampus has also been investigated with fMCI. Synchronous Ca^{2+} transients were correlated with interictal discharges (Badea *et al.*, 2001; Takano

Correspondence: Koichi Ogawa, as above.
E-mail: kouichi.ogawa@shionogi.co.jp

Received 30 January 2014, revised 28 April 2015, accepted 6 May 2015

et al., 2012), which are a common feature of epilepsy in addition to SLEs, and can be identified as transient synchronous events in local field potential recordings, and sustained synchronous Ca^{2+} influx was correlated with SLEs (Gómez-Gonzalo *et al.*, 2010; Cammarota *et al.*, 2013). Cammarota *et al.* (2013) demonstrated that parvalbumin-expressing, fast-spiking interneurons controlled seizure propagation. Interictal events are composed of the variable activity patterns of individual neurons (Sabolek *et al.*, 2012; Feldt Muldoon *et al.*, 2013). Consequently, fMCI studies have begun to reveal the mechanisms and properties of epileptiform events. However, little is known about how antiepileptic drugs act on these individual neurons during epileptiform events. Evaluation of the effects of antiepileptic drugs on these individual cells in the neuronal network will have great potential for novel drug development. In this study, we used fMCI to record the activities of multiple neurons in the CA1 region of the rat hippocampus treated with the proconvulsant bicuculline under Mg^{2+}-free conditions, in addition to using conventional electrophysiological techniques. Bicuculline induced synchronous Ca^{2+} influx that was correlated with SLEs. Several other proconvulsants also induced synchronous Ca^{2+} influx. We considered this synchronous Ca^{2+} influx as a key phenotype of an *in vitro* epilepsy model, and investigated the effects of several antiepileptic drugs (phenytoin, flupirtine, and ethosuximide) that act on different molecular targets on bicuculline-induced synchronous Ca^{2+} influx. Phenytoin is a voltage-dependent and frequency-dependent inhibitor of voltage-dependent Na^+ channels (Mantegazza *et al.*, 2010). Flupirtine is a Kv7.2/7.3 channel opener, and its congener retigabine is prescribed for the treatment of epilepsy (Brown & Passmore, 2009). Ethosuximide is a T-type Ca^{2+} channel inhibitor (Gören & Onat, 2007). We demonstrated that these drugs had heterogeneous effects on the *in vitro* epilepsy model.

Materials and methods

Animal experiments

The experiments were performed on 41 Wistar rats of both sexes at postnatal days 6–8 (SLC, Shizuoka, Japan). The rats were housed under controlled temperature and humidity with a 12 : 12-h light/dark cycle, and allowed access to water and food *ad libitum*. All procedures were approved by the Animal Care and Use Committee of Shionogi Research Laboratories, Osaka, Japan, in agreement with the internal guidelines for animal experiments and in adherence to the ethics policies of Shionogi & Co., Ltd (Osaka, Japan).

Slice preparations

The rats were decapitated, and the brain was immersed in ice-cold modified artificial cerebrospinal fluid (ACSF) consisting of 25 mM $NaHCO_3$, 1.0 mM NaH_2PO_4, 3.0 mM KCl, 5.0 mM $MgCl_2$, 1.0 mM $CaCl_2$, 11 mM glucose, and 215.5 mM sucrose, bubbled with 95% O_2 and 5% CO_2. The hippocampus was isolated and embedded in 3% agarose gel. Transverse hippocampal slices (400 μm) were cut with a vibratome (VT1200S; Leica, Wetzlar, Germany). The slices were maintained for > 40 min at 32 °C in normal ACSF consisting of 113 mM NaCl, 25 mM $NaHCO_3$, 1.0 mM NaH_2PO_4, 3.0 mM KCl, 1.0 mM $MgCl_2$, 2.0 mM $CaCl_2$, and 11 mM glucose, bubbled with 95% O_2 and 5% CO_2.

Calcium imaging

Slices were incubated for 60 min at 32 °C with 0.0005% Oregon Green 488 BAPTA-1AM (OGB-1) (Invitrogen, Carlsbad, CA, USA), 0.01% Pluronic F-127 (Invitrogen), and 0.005% Cremophor EL (Nacalai Tesque, Kyoto, Japan), and were allowed to recover in ACSF for > 40 min. The slices were transferred to a recording chamber perfused with 30–32 °C Mg^{2+}-free ACSF consisting of 113 mM NaCl, 25 mM $NaHCO_3$, 1.0 mM NaH_2PO_4, 3.0 mM KCl, 2.0 mM $CaCl_2$, and 11 mM glucose, bubbled with 95% O_2 and 5% CO_2, at a rate of 2.0 mL/min. After a stabilisation period of 10 min, imaging of spontaneous Ca^{2+} signals in the CA1 region was performed. Images were captured at 11–12 frames/s with a Nipkow disk confocal unit (CSUX1; Yokogawa Electric, Tokyo, Japan), a cooled CCD camera (iXon DU897; Andor Technology, Belfast, UK), an upright microscope (Eclipse FN1; Nikon, Tokyo, Japan), with a water-immersion objective (×16; numerical aperture, 0.80; Nikon), and image acquisition software (Andor iQ; Andor Technology). OGB-1 was excited at 488 nm with a DPSS laser (30 mW, BC-001-B; Melles Griot, Albuquerque, NM, USA). To minimise photobleaching, the intensity of the laser was attenuated to 5% with a neutral density filter.

The cell bodies of neurons were identified by eye to determine the regions of interest in which the average fluorescence was measured. Slices in which > 80 cells were stained by OGB-1 were accepted. For each cell, the change in somatic fluorescence ($\Delta F/F$) was calculated as $(F_1-F_0)/F_0$, where F_1 is the fluorescence intensity at any time point, and F_0 is the average baseline fluorescence intensity. A cell was considered to be active at any time when $\Delta F/F$ was not less than 0.05. The peak, area under the curve (AUC) and duration of the Ca^{2+} signals were calculated with PCLAMP software (Molecular Devices, Sunnyvale, CA, USA).

To assess the effects of antiepileptic drugs on collective behavior in a neuronal network, bicuculline (10 μM) was applied to slices to induce epileptiform events under Mg^{2+}-free conditions, and the antiepileptic drug or ACSF (control group) was applied, starting 1 min after the first bicuculline-induced sustained synchronous Ca^{2+} influx. After the antiepileptic drugs and bicuculline had been applied for 2 min, the effects of the antiepileptic drugs on bicuculline-induced synchronous Ca^{2+} influx were assessed for 15 min. The AUC (i.e. the amount of Ca^{2+} influx) and the peak of the somatic fluorescence trace of bicuculline-induced synchronous Ca^{2+} influx were normalised relative to the average baseline fluorescence intensity. We evaluated two types of indicator: (i) indicators of effects on a synchronous event (peak, AUC, and duration); and (ii) indicators of the total effect during the measurement time (number of events, total AUC, and ratio of active cells). Differences between groups were analysed for statistical significance with Steel's test, and $P < 0.05$ was taken to indicate statistical significance.

To assess changes in bicuculline-induced synchronous events in individual cells before and after application of the antiepileptic drugs, mean peaks of synchronous events 2–10 min before application were compared with those 10 min after application in each individual cell. Correlations between the pre-drug peak and the post-drug/pre-drug peak ratio were assessed by use of the Spearman rank correlation coefficient. The *Z*-test for two correlation coefficients was used to evaluate the difference between the coefficients (Kendall *et al.*, 1994). $P < 0.05$ was taken to indicate statistical significance.

Patch-clamp recording

For loose cell-attached recordings, CA1 pyramidal neurons were visually identified by OGB-1 fluorescence. With simultaneous recording of Ca^{2+} signals, spike activities of a single cell were recorded with borosilicate glass pipettes filled with ACSF

(3–6 MΩ). Data were obtained with an EPC10 (Heka, Darmstadt, Germany) with PULSE software (Heka), and filtered at a cut-off frequency of 2.9 kHz. Spike activity was digitised at 10 kHz with PowerLab (AD Instruments, Dunedin, New Zealand) for computer analysis with LABCHART (AD Instruments).

Local field potential recording

For recording of local field potentials, hippocampal slices were placed in the recording chamber with a 64-planar multielectrode array, each element having a diameter of 50 μm (MED-P50025; Alpha MED Scientific, Osaka, Japan). Local field potentials from the CA1 region were recorded with a multichannel recording system (Cerebus Data Acquisition System; Blackrock Microsystems, Salt Lake City, UT, USA) with a low-cut filter at 0.3 Hz and a high-cut filter at 500 Hz. The signal was digitised at 10 kHz with CENTRAL software (Blackrock Microsystems). For assessment of SLEs, proconvulsants were applied under Mg^{2+}-free conditions. SLEs were detected as synchronous changes in local field potentials followed by after-discharges (Anderson *et al.*, 1986; Nyikos *et al.*, 2003).

After stable recording of SLEs under Mg^{2+}-free/bicuculline conditions, several antiepileptic drugs were applied to assess them. We evaluated the duration and number of SLEs just before and after application of a drug (10 min). Differences between paired groups were analysed for statistical significance with Wilcoxon's signed-rank test, and $P < 0.05$ was taken to indicate statistical significance.

Drugs

Drugs were given via bath application. (−)-Bicuculline methobromide (bicuculline) and 4-aminopyridine (4-AP) were purchased from Wako (Osaka, Japan). Pentylenetetrazole (pentetrazol), 5,5-diphenylhydantoin (phenytoin) and pilocarpine were purchased from Sigma (St Louis, MO, USA). Flupirtine maleate (flupirtine) and ethosuximide were purchased from Tocris Cookson (Bristol, UK) and Tokyo Chemical Industry (Tokyo, Japan), respectively.

Statistics

Differences between multiple groups were analysed for statistical significance with Steel's test. The Mann–Whitney *U*-test was used to compare single parameters between unpaired groups, and Wilcoxon's signed-rank test was used for paired groups. The cumulative distributions of two groups were compared by use of the Kolmogorov–Smirnov test. The Spearman rank correlation coefficient was used to assess the correlation between two parameters of interest. The *Z*-test for two correlation coefficients was used to evaluate the difference between two coefficients, as described above. All data are presented as means ± standard errors of the mean (SEMs). In all analyses, $P < 0.05$ was taken to indicate statistical significance.

Results

Bicuculline induces SLEs

The excitatory–inhibitory balance is thought to be disrupted at the onset of epileptic seizure. γ-Aminobutyric acid (GABA) is recognised as the principal inhibitory neurotransmitter in the central nervous system. Abnormalities of GABAergic function and reduction of GABA-mediated inhibition have often been observed in both epilepsy models and human patients (Ribak *et al.*, 1979; Olsen *et al.*, 1985; McDonald *et al.*, 1991; Henry *et al.*, 1993). Therefore, we first examined the effects of the proconvulsant bicuculline, a $GABA_A$ antagonist, on acute hippocampal slices by using local field potential recordings. Treatment with bicuculline (10 μM) under Mg^{2+}-free conditions induced SLEs in extracellular field potentials in the CA1 region (Fig. 1A). These SLEs were recurrent, and consisted of initial synchronous changes in local field potentials followed by after-discharges lasting for > 10 s, similarly to observations reported previously (Anderson *et al.*, 1986; Nyikos *et al.*, 2003).

Bicuculline induces synchronous Ca^{2+} influx

Simultaneous loose cell-attached recordings and Ca^{2+} imaging in the CA1 region revealed that transient and sustained Ca^{2+} elevations (transient – returned to baseline within several seconds; sustained – lasting for > 10 s) induced by bicuculline (10 μM) under Mg^{2+}-free conditions reflected action potentials and tonic burst firing, respectively (Fig. 1B). On the basis of a previous report (Nyikos *et al.*, 2003), tonic bursts recorded at a single cell are considered to be SLEs in extracellular field potentials. To clarify the collective behavior of multiple neurons, the activities of CA1 neurons were monitored with fMCI (Fig. 1C). We detected 129.9 ± 2.7 neurons per slice in this study (64 slices from 24 rats). The mean photobleaching rate was 1.89 ± 0.13%/min (nine slices from five rats). Treatment with bicuculline (10 μM) under Mg^{2+}-free conditions induced synchronous Ca^{2+} influx in the CA1 region. This synchronous Ca^{2+} influx was recurrent and was accompanied by sustained Ca^{2+} increases (Fig. 1D). Whereas most transient Ca^{2+} activities involved a change in $\Delta F/F$ of 5–20% (shown in blue), the sustained synchronous Ca^{2+} influx involved a large change in $\Delta F/F$ of >30% (shown in red; Fig. 1D, top and middle). For 113 events in nine slices, 99.988 ± 0.009% neurons were recruited per event (1273 neurons). The inter-event interval and event duration of synchronous Ca^{2+} influx were similar to those of the SLEs, and no significant differences were observed between them (interval of SLEs, 136.9 ± 13.9 s, seven slices; interval of Ca^{2+} influx, 95.2 ± 17.2 s, nine slices, $P = 0.0907$, $U = 15$, Mann–Whitney test; duration of SLEs, 26.6 ± 3.6 s, seven slices; duration of Ca^{2+} influx, 20.0 ± 2.4 s, nine slices, $P = 0.2509$, $U = 20$, Mann–Whitney test). Taken together, these results suggest that bicuculline-induced synchronous Ca^{2+} influx in the CA1 region is correlated with SLEs in extracellular recordings.

Other proconvulsants also induce synchronous Ca^{2+} influx and SLEs

To confirm that synchronous Ca^{2+} influx is a common feature observed with other proconvulsants, we examined the effects of several proconvulsants with different mechanisms of action that are used in *in vivo* epilepsy models (Turski *et al.*, 1983; Diehl *et al.*, 1984; Cramer *et al.*, 1994); i.e. 4-AP (K^+ channel blocker), pentetrazol ($GABA_A$ receptor antagonist), and pilocarpine (muscarinic receptor agonist). All of these drugs induced synchronous Ca^{2+} influx in the CA1 region under Mg^{2+}-free conditions (Fig. 2A–D). Figure 2E–H shows several indicators of synchronous events over 25 min, such as the number of events, inter-event interval, event duration, and latency to the first event. These results suggest that all of the proconvulsants, which have different mechanisms of action, induced synchronous Ca^{2+} influx in the same manner as bicuculline. The combination of both a proconvulsant and Mg^{2+}-free ACSF is a severe condition. Treatment only with Mg^{2+}-free ACSF for 40 min did not induce synchronous events, whereas we did detect

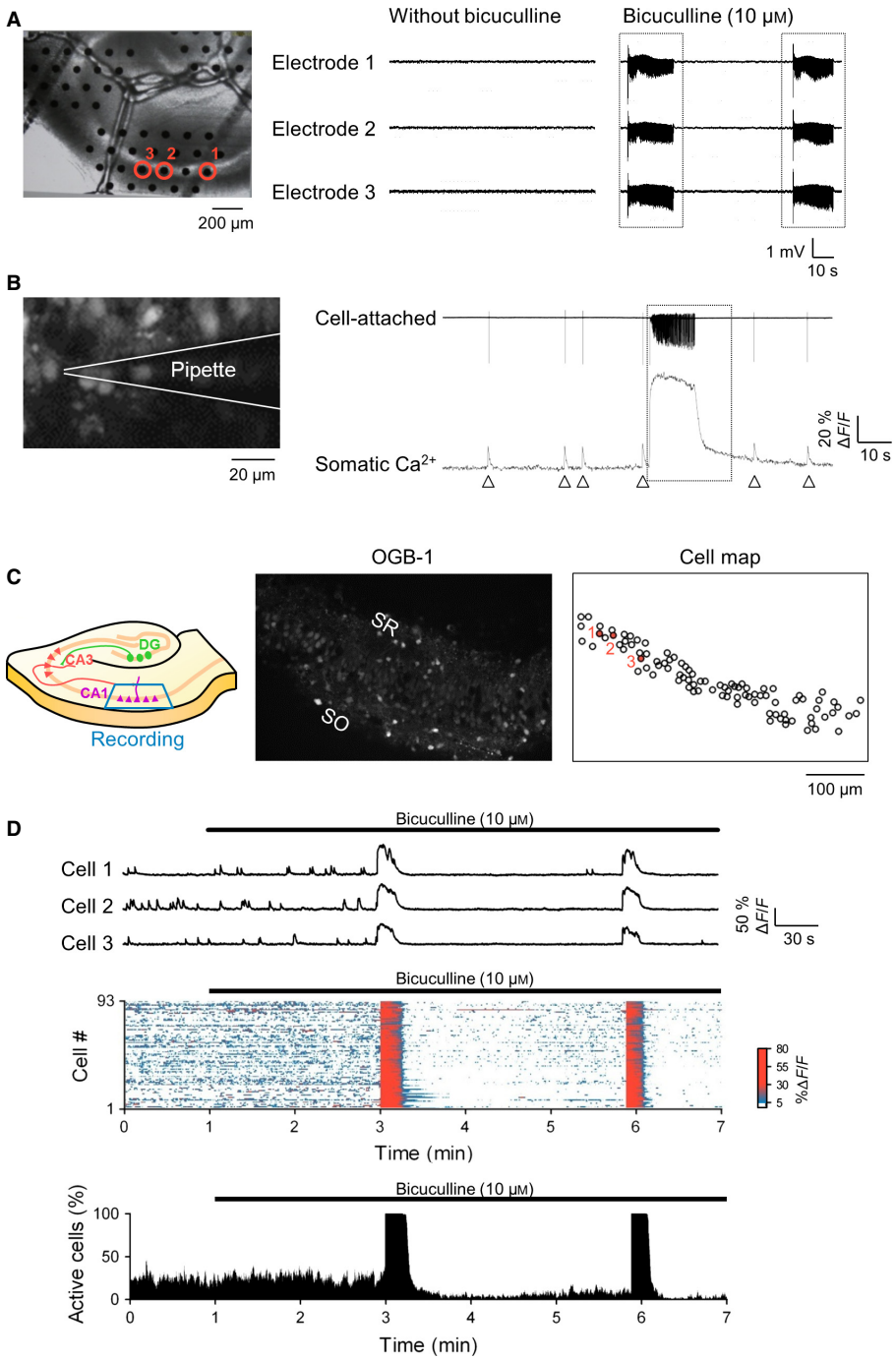

FIG. 1. SLEs and synchronous Ca^{2+} influx were induced by bicuculline (10 μM) in the CA1 region of hippocampal slices. (A) Arrangement of multiple electrodes on the hippocampal slice (left). Representative traces of local field recording in the CA1 pyramidal cell layer with or without bicuculline (10 μM) (middle and right, respectively) show that bicuculline (10 μM) induced SLEs under Mg^{2+}-free conditions (dashed box on the right). (B) Confocal image of the CA1 region of a slice loaded with OGB-1 (left). Simultaneous cell-attached recording and Ca^{2+} imaging revealed that spikes and bursts elicited transient (open arrowheads) and sustained (dashed box) Ca^{2+} elevations in the soma (right). (C) Experimental design of Ca^{2+} imaging to examine activity of the CA1 region in hippocampal slices (left). Confocal image of a slice loaded with OGB-1 (middle). SO, stratum oriens; SR, stratum radiatum. The cell map shows 93 neurons (right). The three representative cells for which the traces are shown in D are indicated with red circles. (D) Bicuculline-induced Ca^{2+} activity in the CA1 region. Raw traces indicate the changes in fluorescence intensity of three representative cells (cells 1, 2, and 3) on the cell map of C (top). Synchronous Ca^{2+} influx was induced within minutes after treatment with bicuculline (10 μM). Synchronous Ca^{2+} influx lasted for > 10 s, and occurred repeatedly. Spontaneous Ca^{2+} activity of a total of 93 cells shows that bicuculline-induced synchronous activity included a large amount of Ca^{2+} influx, shown in red (middle). The color scale indicates the changes in fluorescence intensity. The ratio of active cells to the total number of cells monitored indicated that all of the cells participated in the synchronous events (bottom).

synchronous events with bicuculline alone in normal ACSF for all of the slices recorded (data not shown, five slices from each of five rats). The reason why Mg^{2+}-free ACSF alone did not induce the events might be that ionic manipulation takes longer to cause SLEs than a proconvulsant (Karlócai *et al.*, 2014). Although bicuculline in normal ACSF did induce synchronous events, the combination

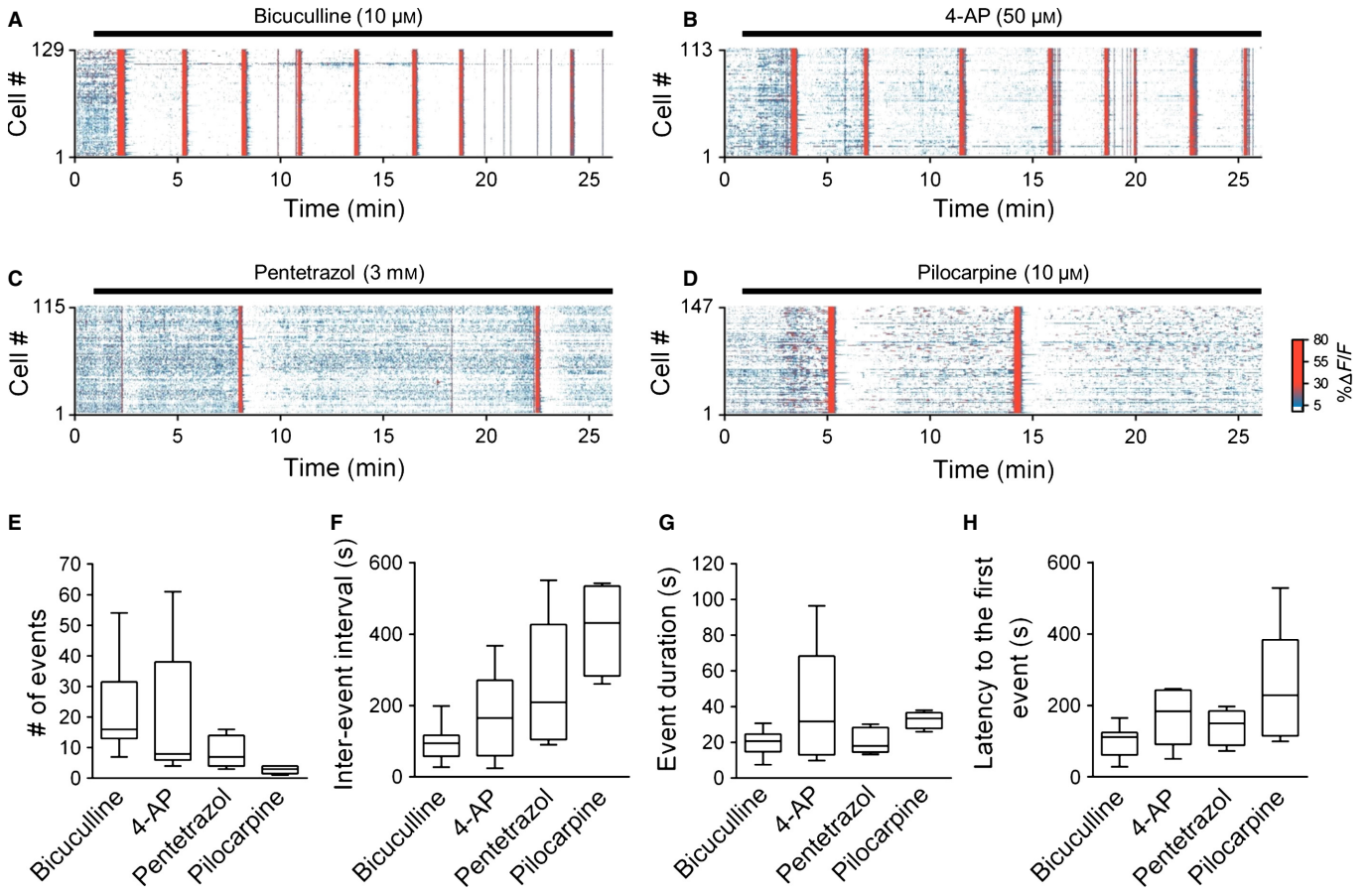

FIG. 2. Several proconvulsants induced synchronous Ca^{2+} influx in the CA1 region. (A–D) Ca^{2+} influx of multiple neurons in the CA1 region treated with bicuculline (10 μM) (A), 4-AP (50 μM) (B), pentetrazol (3 mM) (C), and pilocarpine (10 μM) (D). All of the proconvulsants caused recurrent synchronous Ca^{2+} influxes. (E–H) Several indicators of synchronous Ca^{2+} influx induced by proconvulsants are indicated as box plots: the number of events (E), inter-event interval (F), event duration (G), and latency to the first event (H). Boxes represent the 25th and 75th percentiles; lines inside the boxes are medians; whiskers indicate the minimum and maximum values (bicuculline, nine slices from five rats; 4-AP, five slices from five rats; pentetrazol, five slices from five rats; pilocarpine, five slices from five rats). Regarding the inter-event interval (E), slices in which synchronous events were detected more than once during 25 min were analysed (all of the slices recorded in each group other than pilocarpine, and four of five slices in the pilocarpine group).

induced more synchronous events than bicuculline alone. We chose the combination condition for assessing the antiepileptic drugs so as to minimise photobleaching, because the condition allowed us to perform assessments quickly.

Phenytoin and flupirtine decrease the amount of Ca^{2+} influx, whereas ethosuximide increases the event duration

As we speculated that antiepileptic drugs exert their effects on synchronous Ca^{2+} influx, we applied several such drugs; i.e. phenytoin (a blocker of voltage-dependent Na^+ channels), flupirtine (a Kv7.2/7.3 channel opener; the antiepileptic drug retigabine is a congener of flupirtine), and ethosuximide (a T-type Ca^{2+} channel inhibitor), and examined their effects on bicuculline-induced synchronous Ca^{2+} influx (Fig. 3A). We first compared the effects of these drugs on collective behavior in neuronal networks. This approach allowed us to see the effects of antiepileptic drugs on the distribution of responses of individual cells as a whole, in contrast to conventional approaches, such as local field potential recording, which evaluate the summed activity of multiple neurons. Figure 3B shows the Ca^{2+} influx for all of the cells in the CA1 region and the traces for three representative cells. We compared the peak, AUC and duration of the first synchronous Ca^{2+} influx induced by bicuculline under the Mg^{2+}-free condition in each experiment (ACSF group and antiepileptic drug groups), and no significant differences were observed (data not shown). After the first synchronous Ca^{2+} influx, we applied the antiepileptic drugs, and assessed their effects on bicuculline-induced synchronous Ca^{2+} influx for 15 min. Figure 4A shows plots of the peaks of the Ca^{2+} responses in the synchronous events of individual cells against their AUCs. Different slices are indicated by different colors. As compared with the control slices, the data points of the slices treated with phenytoin and flupirtine are condensed in the lower part of the plots, indicating that these drugs reduced the AUC of the Ca^{2+} responses. The data for the ethosuximide-treated slices tended to be more scattered towards higher AUCs. These data are pooled in Fig. 4B, which illustrates the cumulative distributions of the mean peaks and AUCs of the Ca^{2+} responses (ACSF, 1273 cells in nine slices from five rats; phenytoin, 1123 cells in eight slices from five rats; flupirtine, 1070 cells in eight slices from five rats; ethosuximide, 1118 cells in eight slices from four rats). For both the peaks and AUCs, the distributions of phenytoin and flupirtine were shifted leftwards as compared with the control (Kolmogorov–Smirnov test: control vs. phenytoin in peaks, $D = 0.66$, $P < 0.0001$; control vs. flupirtine in peaks, $D = 0.61$, $P < 0.0001$; control vs. phenytoin in AUCs, $D = 0.80$, $P < 0.0001$; control vs. flupirtine in AUCs, $D = 0.83$, $P < 0.0001$). For the AUC, cells treated with ethosuximide were distributed rightwards as compared with the control, and ethosuximide changed the distribution of peaks slightly (Kolmogorov–Smirnov test: control vs.

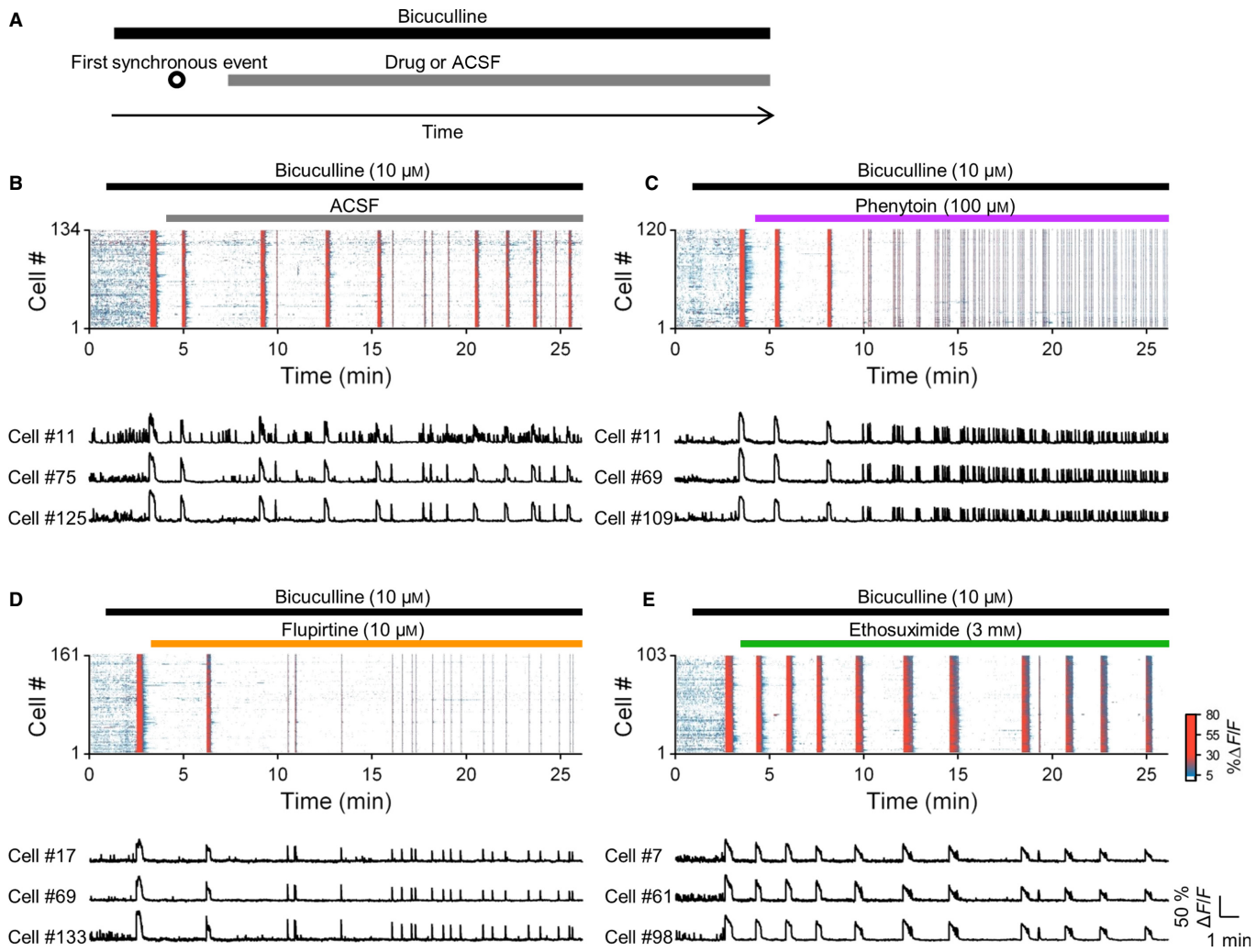

FIG. 3. The effects of antiepileptic drugs on bicuculline-induced synchronous Ca^{2+} influx determined by monitoring the collective behavior of multiple neurons in the CA1 region. (A) Experimental schedules. After the first sustained synchronous event had been observed, antiepileptic drugs or ACSF (control) were applied. In the presence of drugs, bicuculline-induced synchronous events were measured. (B–E) Bicuculline-induced Ca^{2+} influx with the application of ACSF (B, upper), phenytoin (100 μM) (C, upper), flupirtine (10 μM) (D, upper), and ethosuximide (3 mM) (E, upper). Raw traces of the Ca^{2+} signals in three representative cells are indicated at the bottom.

ethosuximide in peaks, $D = 0.062$, $P = 0.021$; control vs. ethosuximide in AUCs, $D = 0.44$, $P < 0.0001$). We used several indicators to quantify the effects of these drugs. To assess the effects on a synchronous event, we used indicators such as the average values of the peak, AUC, and duration per slice; to assess the total effects during the measurement time, we used indicators such as the number of events, total AUC, and ratio of active cells during the events (Fig. 5). Phenytoin and flupirtine decreased the peak and duration (Steel's test: control vs. phenytoin peak, $P = 0.0148$; control vs. flupirtine peak, $P = 0.0081$; control vs. phenytoin duration, $P = 0.0043$; control vs. flupirtine duration, $P = 0.0081$; Fig. 5A and C), and they decreased the AUC drastically (Steel's test: control vs. phenytoin, $P = 0.0022$; control vs. flupirtine, $P = 0.0016$; Fig. 5B). Phenytoin increased the number of synchronous events (Steel's test: control vs. phenytoin, $P = 0.0331$; Fig. 5D). Overall, however, both drugs significantly decreased the total AUC, i.e. total Ca^{2+} influx through synchronous events during the measurement time (Steel's test: control vs. phenytoin, $P = 0.0437$; control vs. flupirtine, $P = 0.0016$; Fig. 5E). In contrast, ethosuximide significantly increased the duration and tended to increase the AUC, although the peak, number of events and total AUC did not change (Steel's test: control vs. ethosuximide duration, $P = 0.0437$; control vs. ethosuximide AUC, $P = 0.0894$; control vs. ethosuximide peak, $P = 0.9952$; control vs. ethosuximide number of events, $P = 0.0859$; control vs. ethosuximide total AUC, $P > 0.9999$; Fig. 5A–E). None of the drugs abolished synchronous events themselves, and, interestingly, the ratio of active cells during synchronous events for the drug groups was not different from that of the ACSF group (Steel's test: control vs. phenytoin, $P = 0.3302$; control vs. flupirtine, $P = 0.9638$; control vs. ethosuximide, $P = 0.3814$; Fig. 5F). These results suggest that phenytoin and flupirtine did not abolish synchronous events themselves, but decreased the amount of Ca^{2+} influx during the events, and that ethosuximide increased the event duration.

The magnitude of phenytoin inhibition of peak synchronous Ca^{2+} influx depends on the peak amplitude of the synchronous event in each cell

As demonstrated above, antiepileptic drugs have heterogeneous effects on collective behavior in neuronal networks. However, it is not known how these drugs affect individual cells (i.e. before and after drug application), or whether there are any distinct populations

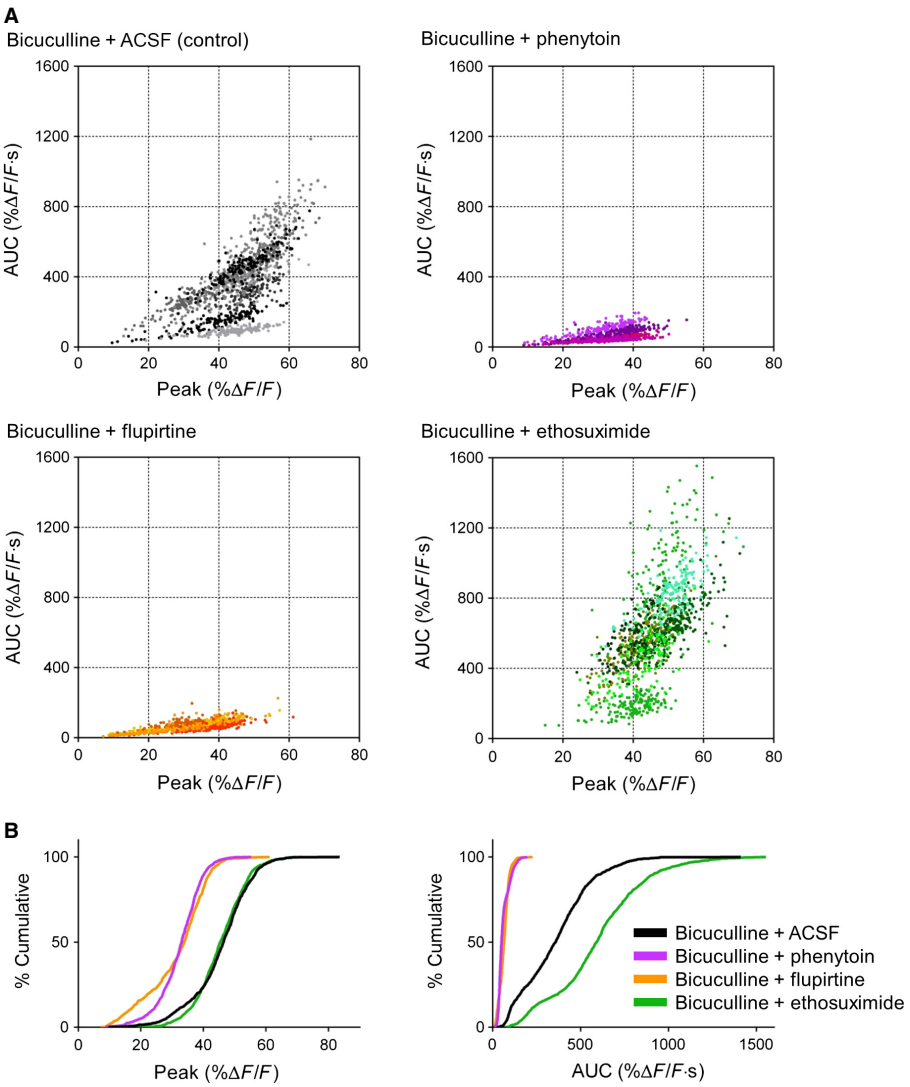

FIG. 4. The effects of antiepileptic drugs on the peak and AUC of individual cells during bicuculline-induced synchronous Ca^{2+} influx in the CA1 region. The peak and AUC of individual cells were assessed by averaging each synchronous event for 15 min. (A) Averaged values of the peak and AUC of individual cells were plotted and color-coded according to slices (upper left, control; upper right, phenytoin; lower left, flupirtine; lower right, ethosuximide). (B) The pooled data of the mean peaks (left) and AUCs (right) were plotted as cumulative distributions (control, 1273 cells in nine slices from five rats; phenytoin, 1123 cells in eight slices from five rats; flupirtine, 1070 cells in eight slices from five rats; ethosuximide, 1118 cells in eight slices from four rats).

that are more susceptible. To address these questions, we evaluated changes in synchronous events 2–10 min before and 10 min after drug application in each individual cell (Fig. 6A and B). We measured peak Ca^{2+} response because it appeared to be less affected by photobleaching during measurement than other indicators (e.g. AUC). Figure 6C shows mean pre-drug peak Ca^{2+} responses during synchronous events in individual cells plotted against the ratios of mean post-drug peaks to mean pre-drug peaks (ACSF, 1119 cells in eight slices from five rats; phenytoin, 1143 cells in eight slices from five rats; flupirtine, 1081 cells in eight slices from six rats; ethosuximide, 1199 cells in nine slices from six rats). Different slices are indicated by different colors. Pre-drug peaks and post-drug peak/pre-drug peaks were negatively correlated in all groups (Spearman rank correlation coefficient R: ACSF, $R = -0.34$, $P < 0.0001$; phenytoin, $R = -0.44$, $P < 0.0001$; flupirtine, $R = -0.18$, $P < 0.0001$; ethosuximide, $R = -0.36$, $P < 0.0001$). The correlation coefficient for phenytoin was significantly lower than those for the control and flupirtine, indicating that cells with large Ca^{2+} responses are more sensitive to phenytoin (Z-test for two correlation coefficients: control vs. phenytoin, $Z = 2.99$, $P = 0.00275$; phenytoin vs. flupirtine, $Z = 7.00$, $P < 0.0001$). The coefficient for flupirtine was closer to zero than that for the control (control vs. flupirtine, $Z = 4.01$, $P < 0.0001$). Correlation coefficients for the control and ethosuximide did not differ (control vs. ethosuximide, $Z = 0.538$, $P = 0.590$).

Phenytoin and flupirtine decrease and ethosuximide increases the duration of SLEs

Finally, we assessed the effects of antiepileptic drugs on SLEs in the CA1 region by using local field recordings, comparing recordings before and after application of a drug (10 min each; Fig. 7A). Phenytoin and flupirtine significantly reduced the duration of SLEs (Wilcoxon's signed-rank test: control vs. phenytoin, $P = 0.0313$; control vs. flupirtine, $P = 0.0313$, Fig. 7B and C), but they did not completely abolish the appearance of SLEs, and, indeed, increased

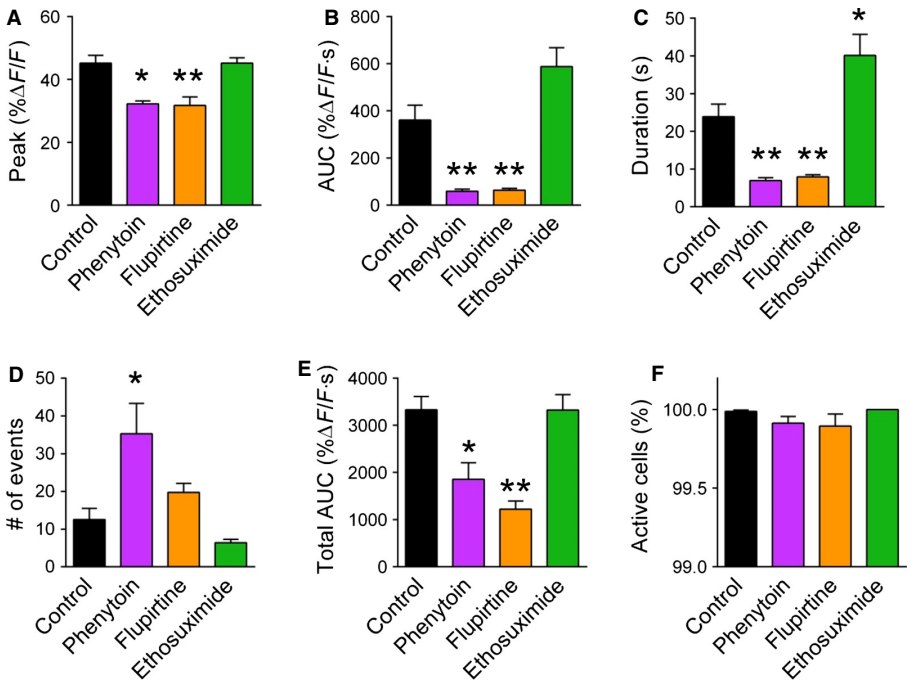

FIG. 5. Phenytoin and flupirtine decreased the amount of Ca^{2+} influx, but ethosuximide increased the event duration, in the CA1 region. (A) Phenytoin and flupirtine decreased the peak of the synchronous Ca^{2+} influx, but ethosuximide did not. (B) Phenytoin and flupirtine decreased the AUC of the synchronous Ca^{2+} influx. Ethosuximide increased the AUC modestly, but the difference was not significant. (C) Phenytoin and flupirtine decreased the event duration, whereas ethosuximide increased it. (D) Phenytoin increased the number of synchronous events. (E) Phenytoin and flupirtine decreased the total AUC, i.e. the total Ca^{2+} influx through synchronous events during the measurement time. (F) None of the drugs changed the ratio of active cells during synchronous events. Asterisks indicate significant differences from the control for each parameter (*$P < 0.05$, **$P < 0.01$, Steel's test). Each column represents the mean ± SEM (eight or nine slices from four or five rats in each group).

the number of events (Wilcoxon's signed-rank test: control vs. phenytoin, $P = 0.0313$; control vs. flupirtine, $P = 0.0313$; Fig. 7B and D). In contrast, ethosuximide significantly increased the duration of SLEs, with no changes in the number of events (Wilcoxon's signed-rank test: control vs. ethosuximide for duration, $P = 0.0313$; control vs. ethosuximide for number of events, $P > 0.9999$; Fig. 7B–D).

Discussion

We monitored the collective behaviors of individual neurons during SLEs in hippocampus sections treated with bicuculline under Mg^{2+}-free conditions by using fMCI, and investigated how antiepileptic drugs act on these individual neurons during epileptiform events. We demonstrated that the antiepileptic drugs phenytoin, flupirtine and ethosuximide exert heterogeneous effects on the *in vitro* epilepsy model.

First, we confirmed that bicuculline induced synchronous Ca^{2+} influx, and that these events were correlated with SLEs. Like bicuculline, a few other proconvulsants, including 4-AP, pentetrazol, and pilocarpine, which have been reported to cause SLEs in *in vitro* epilepsy models (Piredda *et al.*, 1986; Avoli *et al.*, 1993; Rutecki & Yang, 1998), induced synchronous Ca^{2+} influx. We also observed that all of these drugs caused SLEs in extracellular field potentials under Mg^{2+}-free conditions (data not shown: 4-AP, three slices from two rats; pentetrazol, two slices from two rats; pilocarpine, two slices from two rats). In agreement with previous studies, our results suggest that proconvulsant-induced synchronous Ca^{2+} influx is a key phenotype in *in vitro* epilepsy models.

We then investigated the effects of antiepileptic drugs that act on different molecular targets, i.e. phenytoin, flupirtine, and ethosuximide, on bicuculline-induced synchronous Ca^{2+} influx and SLEs. Interestingly, none of the drugs abolished the synchronous Ca^{2+} events themselves. These drugs did not even change the ratio of active cells during synchronous Ca^{2+} influx. Phenytoin and flupirtine decreased several indicators, including the peak, AUC, and duration of synchronous Ca^{2+} influx; the reduction in the AUC was particularly drastic. These results were consistent with the results of pooled data for individual cells; phenytoin and flupirtine shifted the cumulative distributions of the peaks and AUCs of individual cells leftwards as compared with the control. Similar results were obtained with local field potential recording. Phenytoin and flupirtine decreased the duration of SLEs. These results suggest that phenytoin and flupirtine depress the sustained part of the SLEs. They have also been shown to suppress SLEs in several *in vitro* models (Armand *et al.*, 1999, 2000; Dost & Rundfeldt, 2000). The profiles of these drugs might explain why they affect only the sustained part of SLEs. Phenytoin stabilises the inactivated form of voltage-dependent Na^+ channels, although it has low affinity for the channels in the resting state (Mantegazza *et al.*, 2010). Phenytoin appears to bind to the channel during after-discharges in SLEs, and this is correlated with the sustained part of synchronous Ca^{2+} influx. However, phenytoin is expected to be less likely to affect channels in the initial part of SLEs, because the channels shift from the closed to the open form, rather than the inactivated form, at this point. Flupirtine enhances Kv7.2/7.3 channel activity. Kv7 channels contribute to the medium after-hyperpolarization, which serves primarily to control the excitability of neurons lasting 50–200 ms after the action potentials (Storm, 1989; Gu *et al.*, 2005); this property might reflect the slow kinetics of activation. In fact, retigabine, which is a congener of flupirtine, does not affect single action potentials, as opposed to attenuation of higher-frequency or burst firing evoked by prolonged depolarizing stimuli (Yue & Yaari, 2004). This might explain why

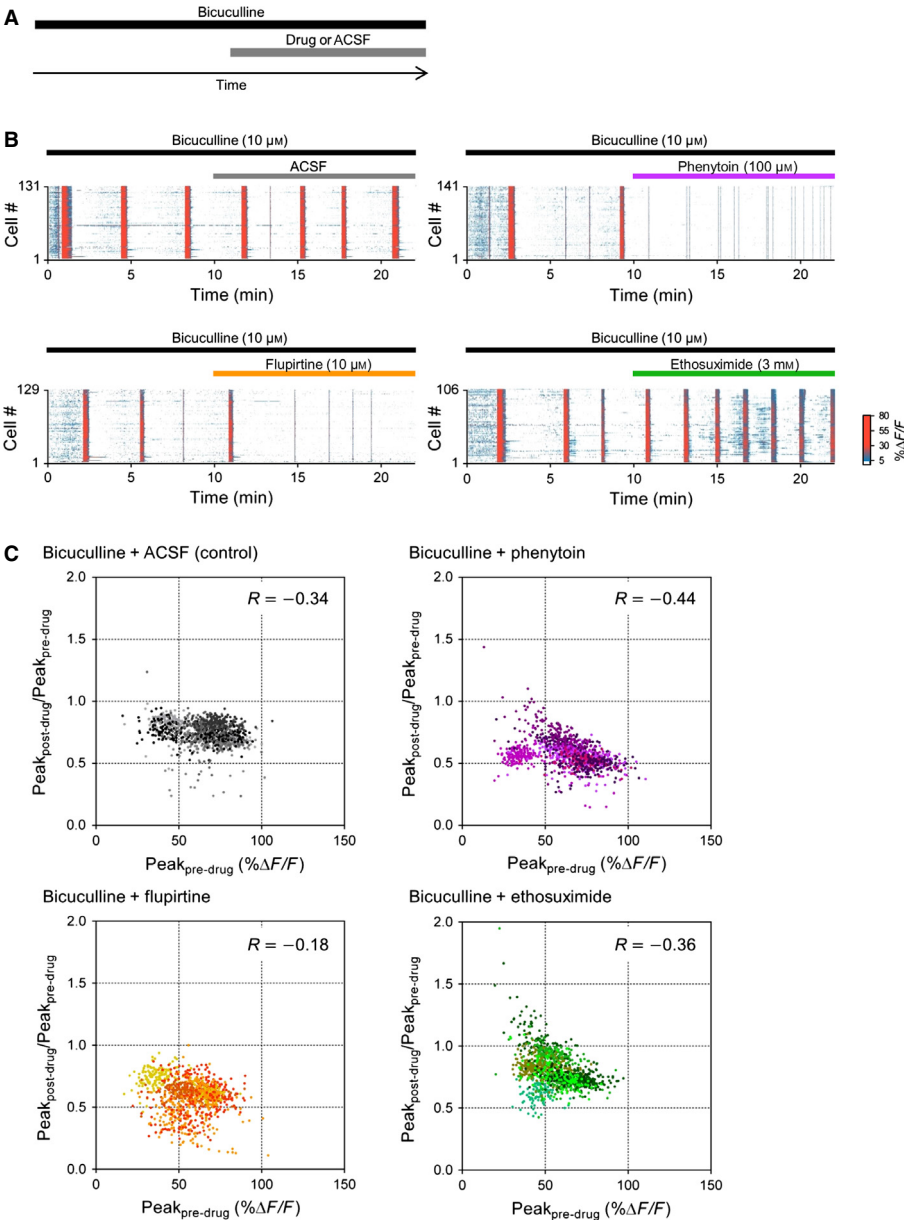

FIG. 6. The magnitude of phenytoin inhibition of peak synchronous Ca^{2+} influx depends on the peak amplitude of the synchronous event in each individual cell. (A) Experimental schedules. The mean peak Ca^{2+} influxes during synchronous events were assessed 2–10 min before and 10 min after drug application in individual cells. (B) Bicuculline-induced Ca^{2+} influx before and after application of ACSF (upper left), phenytoin (100 μM) (upper right), flupirtine (10 μM) (lower left), and ethosuximide (3 mM) (lower right). (C) Mean pre-drug peaks and post-drug peak/pre-drug peak ratios of individual cells were plotted and color-coded according to slices (Spearman rank correlation coefficient: upper left, control, $R = -0.34$, 1119 cells in eight slices from five rats; upper right, phenytoin, $R = -0.44$, 1143 cells in eight slices from five rats; lower left, flupirtine, $R = -0.18$, 1081 cells in eight slices from six rats; lower right, ethosuximide, $R = -0.36$, 1199 cells in nine slices from six rats). The Spearman rank correlation coefficient for phenytoin was significantly lower than those for controls and flupirtine, indicating that cells with high Ca^{2+} influx are more sensitive to phenytoin (*Z*-test for two correlation coefficients: control vs. phenytoin, $Z = 2.99$, $P = 0.00275$; phenytoin vs. flupirtine, $Z = 7.00$, $P < 0.0001$).

flupirtine decreased only the sustained part of the SLEs. Therefore, we suspect that phenytoin and flupirtine decreased the sustained part of the SLEs without altering the ratio of active cells; i.e. synchronisation itself.

We clarified the differences between phenytoin and flupirtine in terms of their effects on the number of events and cell susceptibility. Interestingly, phenytoin significantly increased the number of both synchronous Ca^{2+} influxes and SLEs. Flupirtine also increased the number of SLEs, although the effect was modest, and no significant differences were observed in the number of synchronous Ca^{2+} influxes. This might be attributable to two factors: a property of bicuculline-induced epileptiform events, and a difference in the profiles of phenytoin and flupirtine. First, in bicuculline-induced synchronisation (ACSF group in Fig. 3B), the AUC of an event was positively correlated with the interval between one event and the next (Spearman rank correlation coefficient: $R = 0.68$, $P < 0.0001$, 113 events, nine slices from five rats). This means that synchronous events occur more frequently when the AUC is small. From this, we suspect that inhibition of the sustained part of SLEs by an antiepileptic drug is likely to promote an increase in the number of

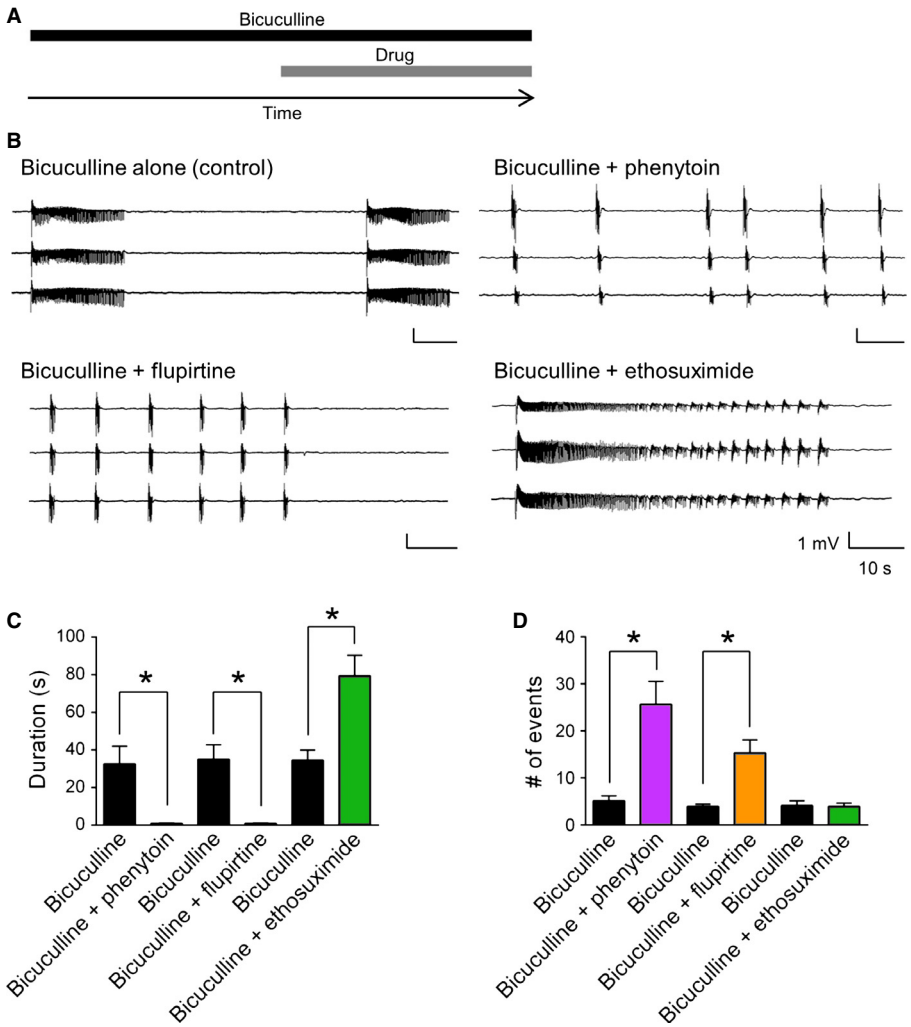

FIG. 7. Phenytoin and flupirtine decreased and ethosuximide increased the duration of SLEs in the CA1 region. (A) Experimental schedules of local field potential recording. After stable recording of bicuculline-induced SLEs, antiepileptic drugs were applied. The average duration and number of SLEs were assessed for 10 min before and after drug applications. (B) Representative traces of local field potentials during bicuculline (10 μM)-induced SLEs in the CA1 region after additional treatment with phenytoin (100 μM) (upper right), flupirtine (10 μM) (lower left), and ethosuximide (3 mM) (lower right). The control trace (bicuculline alone) is shown on the upper left. (C) Phenytoin and flupirtine decreased the duration of SLEs, whereas ethosuximide increased it. (D) Phenytoin and flupirtine increased the number of SLEs. Asterisks indicate significant differences from the respective control groups (*$P < 0.05$, Wilcoxon's signed-rank test). Each column represents the mean ± SEM (six slices from four to six rats in each group).

events, unless the drug also inhibits the neuronal activity during the inter-event intervals. For the second factor, it is reasonable to assume that phenytoin does not improve the excitatory–inhibitory balance in the inter-event intervals, because a large proportion of the Na^+ channels are thought to be in the closed form in the resting state, in which the neuronal firing rate is much lower than the rate of SLEs, and phenytoin would not affect these channels. According to this hypothesis, phenytoin not only decreased the AUC, but also increased the number of events. Flupirtine hyperpolarizes the resting membrane potential (Wladyka & Kunze, 2006). The increase in the number of events caused by AUC inhibition is probably weakened by the stabilisation of the resting membrane potential during the inter-event intervals. Therefore, flupirtine exerted a modest effect on the number of events. Although both phenytoin and flupirtine increased the number of SLEs, they significantly decreased the total AUC, i.e. the summation of the Ca^{2+} influxes during synchronous events.

In addition to the difference in the number of events, phenytoin differed from flupirtine in that it had non-uniform effects depending on the peak amplitude of the synchronous event in each individual cell. In this analysis, photobleaching might have caused the negative correlation between peak Ca^{2+} response and the ratio between that value and the drug effect even in control cells, because large peak responses tend to promote photobleaching. This correlation was more negative for phenytoin than for controls, suggesting that phenytoin is more effective for cells with strong Ca^{2+} responses. This result is reasonable, because phenytoin has a state-dependent effect, as mentioned above, and is thus likely to have strong effects on cells whose firing rates are high. In contrast to what was found for phenytoin, correlations for flupirtine were weaker than for controls, which might indicate that flupirtine's effects are not state-dependent, or that the influence of photobleaching was less than in control cells because of lower synchronous Ca^{2+} influx.

Unlike phenytoin and flupirtine, ethosuximide significantly increased the duration of synchronous Ca^{2+} influx and SLEs, and tended to increase the AUC. In agreement with these results, ethosuximide shifted the cumulative distribution of AUCs of individual cells rightwards as compared with the control. Not

surprisingly, ethosuximide did not decrease the AUC or duration, because it is approved for the treatment of absence seizures and exerts its anti-absence effects by reducing T-type Ca^{2+} currents in thalamocortical relay neurons. When ethosuximide is used for tonic–clonic seizures, it might aggravate the condition in some patients (Perucca *et al.*, 1998). Ethosuximide also enhanced afterdischarge generation in an *in vitro* temporal lobe epilepsy model, although at a relatively high concentration (Ohno & Higashima, 2002). Furthermore, Kobayashi *et al.* (2009) reported that ethosuximide inhibits G-protein-activated inwardly rectifying K^+ channels at clinically relevant concentrations, and proposed that the effect on G-protein-activated inwardly rectifying K^+ channels may be related to aggravation of the symptoms of tonic–clonic seizure patients. The increases in the AUC and duration observed in this study might reflect this side effect.

We studied postnatal day 6–8 rats. This age could create a serious problem for evaluating the function of neuronal networks, because the maturity of the brain is age-dependent. For example, GABA is the major inhibitory neurotransmitter in the adult brain, but, at early postnatal ages, $GABA_A$ receptor activation triggers depolarization of the neuronal membrane, because the neurons have a higher intracellular chloride concentration at these ages, owing to immature expression of transmembrane chloride transporters, and chloride-permeable GABAergic transmission via $GABA_A$ channels therefore has an excitatory effect (Cherubini *et al.*, 1991). Giant depolarizing potentials, which are characterised by spontaneous synchronous network bursts, are often observed at these ages (Ben-Ari *et al.*, 1989, 2007). It has also been reported that GABA-mediated excitation in the developing hippocampus contributes to the initiation of ictal epileptiform activity (Dzhala & Staley, 2003). On the other hand, fMCI is usually performed on juvenile tissue, because of the difficulty of loading adult tissue with Ca^{2+} dyes (Namiki & Ikegaya, 2009); we used postnatal day 6–8 animals to overcome this problem. GABA seemed to at least have an inhibitory effect in this study, because the giant depolarizing potential and epileptiform activity described above were inhibited by the $GABA_A$ antagonist bicuculline, whereas synchronous activity in this study was caused by bicuculline. Therefore, we achieved a good balance between neuronal network maturation and experimental feasibility.

We examined the effects of antiepileptic drugs under GABAergic transmission blockade by bicuculline. Several studies have shown that GABAergic input facilitates after-discharges in SLEs (Köhling *et al.*, 2000; Fujiwara-Tsukamoto *et al.*, 2003, 2006), probably because of the excitatory effects of GABA in adult animals under conditions in which $GABA_A$ receptors are intensely activated (Staley *et al.*, 1995; Taira *et al.*, 1997). Further studies using other proconvulsants, such as 4-AP and pilocarpine, and other *in vitro* models, such as low Ca^{2+}, high K^+, and electrical induction, are needed to determine the precise mechanisms of action of antiepileptic drugs.

In conclusion, using fMCI, we demonstrated heterogeneous effects of antiepileptic drugs on bicuculline-induced synchronous Ca^{2+} influx in the rat hippocampal CA1 region. Phenytoin and flupirtine decreased the AUC, peak and duration of synchronous Ca^{2+} influx, and the duration of SLEs, whereas they did not eliminate the synchronous events themselves, or even change the ratio of active cells during events. Ethosuximide increased the duration of synchronous Ca^{2+} influx and SLEs. Furthermore, we found that the magnitude of phenytoin inhibition of peak synchronous Ca^{2+} influx depended on the peak amplitude of the synchronous event in each individual cell. Assessment of antiepileptic drugs with fMCI is a useful tool for developing new drugs.

Abbreviations

4-AP, 4-aminopyridine; ACSF, artificial cerebrospinal fluid; AUC, area under the curve; fMCI, functional multineuron Ca^{2+} imaging; GABA, γ-aminobutyric acid; OGB-1, Oregon Green 488 BAPTA-1AM; SEM, standard error of the mean; SLE, seizure-like event.

References

Albus, K., Wahab, A. & Heinemann, U. (2012) Primary afterdischarge in organotypic hippocampal slice cultures: effects of standard antiepileptic drugs. *Epilepsia*, **53**, 1928–1936.

Anderson, W.W., Lewis, D.V., Swartzwelder, H.S. & Wilson, W.A. (1986) Magnesium-free medium activates seizure-like events in the rat hippocampal slice. *Brain Res.*, **398**, 215–219.

Armand, V., Rundfeldt, C. & Heinemann, U. (1999) Effects of retigabine (D-23129) on different patterns of epileptiform activity induced by 4-aminopyridine in rat entorhinal cortex hippocampal slices. *N.-S. Arch. Pharmacol.*, **359**, 33–39.

Armand, V., Rundfeldt, C. & Heinemann, U. (2000) Effects of retigabine (D-23129) on different patterns of epileptiform activity induced by low magnesium in rat entorhinal cortex hippocampal slices. *Epilepsia*, **41**, 28–33.

Avoli, M., Psarropoulou, C., Tancredi, V. & Fueta, Y. (1993) On the synchronous activity induced by 4-aminopyridine in the CA3 subfield of juvenile rat hippocampus. *J. Neurophysiol.*, **70**, 1018–1029.

Badea, T., Goldberg, J., Mao, B. & Yuste, R. (2001) Calcium imaging of epileptiform events with single-cell resolution. *J. Neurobiol.*, **48**, 215–227.

Ben-Ari, Y., Cherubini, E., Corradetti, R. & Gaiarsa, J.L. (1989) Giant synaptic potentials in immature rat CA3 hippocampal neurones. *J. Physiol.*, **416**, 303–325.

Ben-Ari, Y., Gaiarsa, J.L., Tyzio, R. & Khazipov, R. (2007) GABA: a pioneer transmitter that excites immature neurons and generates primitive oscillations. *Physiol. Rev.*, **87**, 1215–1284.

Bonifazi, P., Goldin, M., Picardo, M.A., Jorquera, I., Cattani, A., Bianconi, G., Represa, A., Ben-Ari, Y. & Cossart, R. (2009) GABAergic hub neurons orchestrate synchrony in developing hippocampal networks. *Science*, **326**, 1419–1424.

Borck, C. & Jefferys, J.G. (1999) Seizure-like events in disinhibited ventral slices of adult rat hippocampus. *J. Neurophysiol.*, **82**, 2130–2142.

Brown, D.A. & Passmore, G.M. (2009) Neural KCNQ (Kv7) channels. *Brit. J. Pharmacol.*, **156**, 1185–1195.

Cammarota, M., Losi, G., Chiavegato, A., Zonta, M. & Carmignoto, G. (2013) Fast spiking interneuron control of seizure propagation in a cortical slice model of focal epilepsy. *J. Physiol.*, **591**(Pt 4), 807–822.

Cherubini, E., Gaiarsa, J.L. & Ben-Ari, Y. (1991) GABA: an excitatory transmitter in early postnatal life. *Trends Neurosci.*, **14**, 515–519.

Cossart, R., Aronov, D. & Yuste, R. (2003) Attractor dynamics of network UP states in the neocortex. *Nature*, **423**, 283–288.

Cossart, R., Ikegaya, Y. & Yuste, R. (2005) Calcium imaging of cortical networks dynamics. *Cell Calcium*, **37**, 451–457.

Cramer, C.L., Stagnitto, M.L., Knowles, M.A. & Palmer, G.C. (1994) Kainic acid and 4-aminopyridine seizure models in mice: evaluation of efficacy of anti-epileptic agents and calcium antagonists. *Life Sci.*, **54**, PL271–PL275.

Diehl, R.G., Smialowski, A. & Gotwo, T. (1984) Development and persistence of kindled seizures after repeated injections of pentylenetetrazol in rats and guinea pigs. *Epilepsia*, **25**, 506–510.

Dost, R. & Rundfeldt, C. (2000) The anticonvulsant retigabine potently suppresses epileptiform discharges in the low Ca^{++} and low Mg^{++} model in the hippocampal slice preparation. *Epilepsy Res.*, **38**, 53–66.

Dzhala, V.I. & Staley, K.J. (2003) Excitatory actions of endogenously released GABA contribute to initiation of ictal epileptiform activity in the developing hippocampus. *J. Neurosci.*, **23**, 1840–1846.

Feldt Muldoon, S., Soltesz, I. & Cossart, R. (2013) Spatially clustered neuronal assemblies comprise the microstructure of synchrony in chronically epileptic networks. *Proc. Natl. Acad. Sci. USA*, **110**, 3567–3572.

Fueta, Y. & Avoli, M. (1992) Effects of antiepileptic drugs on 4-aminopyridine-induced epileptiform activity in young and adult rat hippocampus. *Epilepsy Res.*, **12**, 207–215.

Fujiwara-Tsukamoto, Y., Isomura, Y., Nambu, A. & Takada, M. (2003) Excitatory GABA input directly drives seizure-like rhythmic synchronization in mature hippocampal CA1 pyramidal cells. *Neuroscience*, **119**, 265–275.

Fujiwara-Tsukamoto, Y., Isomura, Y. & Takada, M. (2006) Comparable GABAergic mechanisms of hippocampal seizurelike activity in posttetanic and low-Mg^{2+} conditions. *J. Neurophysiol.*, **95**, 2013–2019.

Gómez-Gonzalo, M., Losi, G., Chiavegato, A., Zonta, M., Cammarota, M., Brondi, M., Vetri, F., Uva, L., Pozzan, T., de Curtis, M., Ratto, G.M. & Carmignoto, G. (2010) An excitatory loop with astrocytes contributes to drive neurons to seizure threshold. *PLoS Biol.*, **8**, e1000352.

Gören, M.Z. & Onat, F. (2007) Ethosuximide: from bench to bedside. *CNS Drug Rev.*, **13**, 224–239.

Gu, N., Vervaeke, K., Hu, H. & Storm, J.F. (2005) Kv7/KCNQ/M and HCN/h, but not KCa2/SK channels, contribute to the somatic medium after-hyperpolarization and excitability control in CA1 hippocampal pyramidal cells. *J. Physiol.*, **566**(Pt 3), 689–715.

Henry, T.R., Frey, K.A., Sackellares, J.C., Gilman, S., Koeppe, R.A., Brunberg, J.A., Ross, D.A., Berent, S., Young, A.B. & Kuhl, D.E. (1993) In vivo cerebral metabolism and central benzodiazepine-receptor binding in temporal lobe epilepsy. *Neurology*, **43**, 1998–2006.

Ikegaya, Y., Aaron, G., Cossart, R., Aronov, D., Lampl, I., Ferster, D. & Yuste, R. (2004) Synfire chains and cortical songs: temporal modules of cortical activity. *Science*, **304**, 559–564.

Jefferys, J.G. & Haas, H.L. (1982) Synchronized bursting of CA1 hippocampal pyramidal cells in the absence of synaptic transmission. *Nature*, **300**, 448–450.

Karlócai, M.R., Kohus, Z., Káli, S., Ulbert, I., Szabó, G., Máté, Z., Freund, T.F. & Gulyás, A.I. (2014) Physiological sharp wave-ripples and interictal events in vitro: what's the difference? *Brain*, **137**(Pt 2), 463–485.

Kendall, M.G., Stuart, A., Ord, J.K., Arnold, S.F. & O'Hagan, A. (1994) *Kendall's Advanced Theory of Statistics*, 6th Edn. Halsted Press, New York.

Kobayashi, T., Hirai, H., Iino, M., Fuse, I., Mitsumura, K., Washiyama, K., Kasai, S. & Ikeda, K. (2009) Inhibitory effects of the antiepileptic drug ethosuximide on G protein-activated inwardly rectifying K^+ channels. *Neuropharmacology*, **56**, 499–506.

Köhling, R., Vreugdenhil, M., Bracci, E. & Jefferys, J.G. (2000) Ictal epileptiform activity is facilitated by hippocampal GABAA receptor-mediated oscillations. *J. Neurosci.*, **20**, 6820–6829.

Korn, S.J., Giacchino, J.L., Chamberlin, N.L. & Dingledine, R. (1987) Epileptiform burst activity induced by potassium in the hippocampus and its regulation by GABA-mediated inhibition. *J. Neurophysiol.*, **57**, 325–340.

Leschinger, A., Stabel, J., Igelmund, P. & Heinemann, U. (1993) Pharmacological and electrographic properties of epileptiform activity induced by elevated K^+ and lowered Ca^{2+} and Mg^{2+} concentration in rat hippocampal slices. *Exp. Brain Res.*, **96**, 230–240.

Mantegazza, M., Curia, G., Biagini, G., Ragsdale, D.S. & Avoli, M. (2010) Voltage-gated sodium channels as therapeutic targets in epilepsy and other neurological disorders. *Lancet Neurol.*, **9**, 413–424.

McDonald, J.W., Garofalo, E.A., Hood, T., Sackellares, J.C., Gilman, S., McKeever, P.E., Troncoso, J.C. & Johnston, M.V. (1991) Altered excitatory and inhibitory amino acid receptor binding in hippocampus of patients with temporal lobe epilepsy. *Ann. Neurol.*, **29**, 529–541.

Mody, I., Lambert, J.D. & Heinemann, U. (1987) Low extracellular magnesium induces epileptiform activity and spreading depression in rat hippocampal slices. *J. Neurophysiol.*, **57**, 869–888.

Namiki, S. & Ikegaya, Y. (2009) Current application and technology of functional multineuron calcium imaging. *Biol. Pharm. Bull.*, **32**, 1–9.

Nyikos, L., Lasztóczi, B., Antal, K., Kovács, R. & Kardos, J. (2003) Desynchronisation of spontaneously recurrent experimental seizures proceeds with a single rhythm. *Neuroscience*, **121**, 705–717.

Ohno, K. & Higashima, M. (2002) Effects of antiepileptic drugs on afterdischarge generation in rat hippocampal slices. *Brain Res.*, **924**, 39–45.

Olsen, R.W., Wamsley, J.K., McCabe, R.T., Lee, R.J. & Lomax, P. (1985) Benzodiazepine/gamma-aminobutyric acid receptor deficit in the midbrain of the seizure-susceptible gerbil. *Proc. Natl. Acad. Sci. USA*, **82**, 6701–6705.

Perucca, E., Gram, L., Avanzini, G. & Dulac, O. (1998) Antiepileptic drugs as a cause of worsening seizures. *Epilepsia*, **39**, 5–17.

Piredda, S., Yonekawa, W., Whittingham, T.S. & Kupferberg, H.J. (1986) Effects of antiepileptic drugs on pentylenetetrazole-induced epileptiform activity in the in vitro hippocampus. *Epilepsia*, **27**, 341–346.

Ribak, C.E., Harris, A.B., Vaughn, J.E. & Roberts, E. (1979) Inhibitory, GABAergic nerve terminals decrease at sites of focal epilepsy. *Science*, **205**, 211–214.

Rutecki, P.A. & Yang, Y. (1998) Ictal epileptiform activity in the CA3 region of hippocampal slices produced by pilocarpine. *J. Neurophysiol.*, **79**, 3019–3029.

Sabolek, H.R., Swiercz, W.B., Lillis, K.P., Cash, S.S., Huberfeld, G., Zhao, G., Ste Marie, L., Clemenceau, S., Barsh, G., Miles, R. & Staley, K.J. (2012) A candidate mechanism underlying the variance of interictal spike propagation. *J. Neurosci.*, **32**, 3009–3021.

Sasaki, T., Matsuki, N. & Ikegaya, Y. (2007) Metastability of active CA3 networks. *J. Neurosci.*, **27**, 517–528.

Smetters, D., Majewska, A. & Yuste, R. (1999) Detecting action potentials in neuronal populations with calcium imaging. *Methods*, **18**, 215–221.

Staley, K.J., Soldo, B.L. & Proctor, W.R. (1995) Ionic mechanisms of neuronal excitation by inhibitory GABAA receptors. *Science*, **269**, 977–981.

Stasheff, S.F., Bragdon, A.C. & Wilson, W.A. (1985) Induction of epileptiform activity in hippocampal slices by trains of electrical stimuli. *Brain Res.*, **344**, 296–302.

Storm, J.F. (1989) An after-hyperpolarization of medium duration in rat hippocampal pyramidal cells. *J. Physiol.*, **409**, 171–190.

Taira, T., Lamsa, K. & Kaila, K. (1997) Posttetanic excitation mediated by GABA(A) receptors in rat CA1 pyramidal neurons. *J. Neurophysiol.*, **77**, 2213–2218.

Takahashi, N., Sasaki, T., Usami, A., Matsuki, N. & Ikegaya, Y. (2007) Watching neuronal circuit dynamics through functional multineuron calcium imaging (fMCI). *Neurosci. Res.*, **58**, 219–225.

Takahashi, N., Takahara, Y., Ishikawa, D., Matsuki, N. & Ikegaya, Y. (2010) Functional multineuron calcium imaging for systems pharmacology. *Anal. Bioanal. Chem.*, **398**, 211–218.

Takano, H., McCartney, M., Ortinski, P.I., Yue, C., Putt, M.E. & Coulter, D.A. (2012) Deterministic and stochastic neuronal contributions to distinct synchronous CA3 network bursts. *J. Neurosci.*, **32**, 4743–4754.

Taylor, C.P. & Dudek, F.E. (1982) Synchronous neural afterdischarges in rat hippocampal slices without active chemical synapses. *Science*, **218**, 810–812.

Traynelis, S.F. & Dingledine, R. (1988) Potassium-induced spontaneous electrographic seizures in the rat hippocampal slice. *J. Neurophysiol.*, **59**, 259–276.

Turski, W.A., Cavalheiro, E.A., Schwarz, M., Czuczwar, S.J., Kleinrok, Z. & Turski, L. (1983) Limbic seizures produced by pilocarpine in rats: behavioural, electroencephalographic and neuropathological study. *Behav. Brain Res.*, **9**, 315–335.

Wladyka, C.L. & Kunze, D.L. (2006) KCNQ/M-currents contribute to the resting membrane potential in rat visceral sensory neurons. *J. Physiol.*, **575**(Pt 1), 175–189.

Yue, C. & Yaari, Y. (2004) KCNQ/M channels control spike afterdepolarization and burst generation in hippocampal neurons. *J. Neurosci.*, **24**, 4614–4624.